Chapter 12 in the book:
P.A. Kralchevsky and K. Nagayama, "Particles at Fluid Interfaces and Membranes"
(Attachment of Colloid Particles and Proteins to Interfaces and Formation of Two-Dimensional Arrays)
Elsevier, Amsterdam, 2001; pp. 503-516.

CHAPTER 12

CAPILLARY FORCES BETWEEN PARTICLES OF IRREGULAR CONTACT LINE

Solid particles attached to a fluid interface often exhibit irregular wetting perimeter. The latter induces interfacial deformations, which are theoretically found to engender a strong lateral capillary force between the particles. For the time being this force is not investigated experimentally, although there are some indications about its existence.

A quantitative theoretical description of such capillary interactions can be achieved for irregularities of a given characteristic amplitude and period, which can be approximated with a model sinusoidal contact line. The latter disturbs the smoothness of the fluid interface creating a wave-like profile. The overlap of the disturbances produced by two particles gives rise to the capillary interaction, which becomes significant for distances comparable with, or smaller than, the wavelength of the contact-line undulation. If the phase shift between the two sinusoidal contact lines is not too large, the interaction is always attractive at long distances between the particles. On the other hand, at short distances the interaction is always repulsive. Only in the special case of coinciding wavelengths and amplitudes the particles attract each other at all distances. The interaction energy exhibits a minimum at some interparticle separation. The depth of the minimum could be greater than the thermal energy kT even if the contact-line undulations have nanometer amplitude. The latter fact implies that this type of capillary force could be significant even for colloid nano-particles and protein macromolecules.

Any deformation of a particulate adsorption monolayer, either by dilatation or by shear, which takes the particles out of the potential minimum, is resisted. As a result, the particle monolayer exhibits dilatational and shear elasticity. These elastic properties can be estimated if the average value and the dispersion of the amplitude of the contact-line undulations are known.

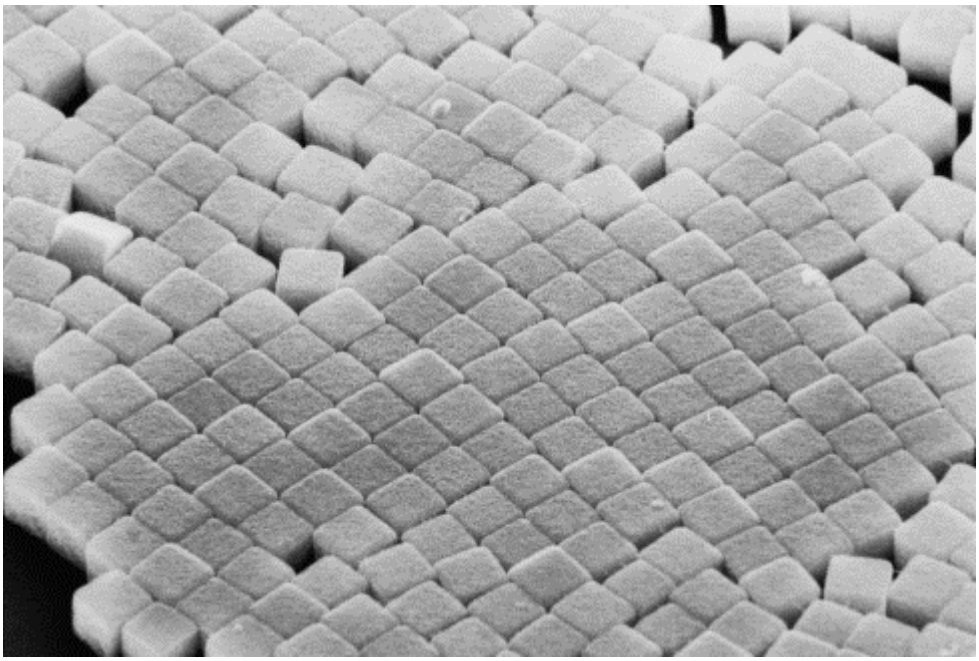

(a)

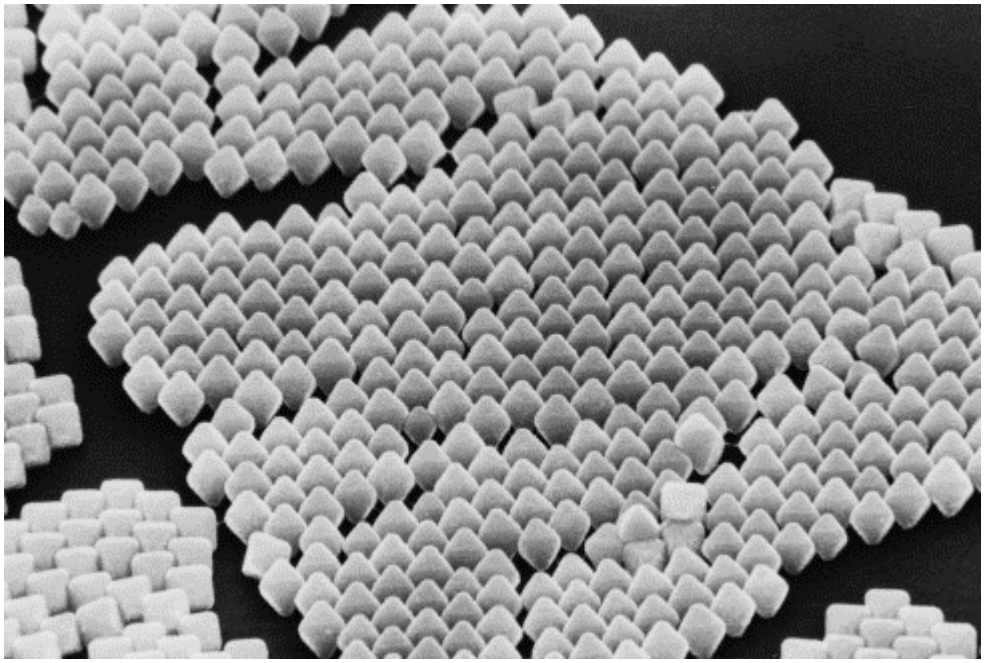

(b)

Fig. 12.1. Electron micrographs: ordered monolayers made of μm-sized crystals (a) from *hexahedral* silver bromide, (b) from *octahedral* silver bromide. The monolayers were initially formed at the water-air interface, then transferred to a mica support and observed by a scanning electron microscope by Heki and Inoue [2] (reprinted with permission).

12.1. SURFACE CORRUGATIONS AND INTERACTION BETWEEN TWO PARTICLES

12.1.1. INTERFACIAL DEFORMATION DUE TO IRREGULAR CONTACT LINE

As discussed in Chapter 8, if the weight of a floating particle is smaller than 5-10 μm, it is not able to create any physically significant interfacial deformation; therefore the lateral flotation force is negligible for such particles. This conclusion holds for spherical particles of regular (smooth) wetting perimeter. Lucassen [1] pointed out that even submicrometer floating particles can create interfacial deformation if the wetting perimeter is not fully located in the plane of the surface, i.e. there are some irregularities of the contact line. Often this is the practical situation with solid particles having some surface roughness and/or inhomogeneity. In the case of crystal particles the contact line can be attached to some jagged edge on the particle surface. Qualitatively, it is to be expected that capillary interaction will appear as soon as the deformed zones around two such particles overlap.

Capillary interaction of this type seems to be rather universal and significant, and it astonishes that for the time being the only study in this area is the work by Lucassen [1]. At least in part, this can be attributed to the impossibility to obtain a quantitative theoretical description, or reproducible experimental data, for particles of completely irregular periphery. Lucassen has overcome this difficulty considering irregularities of given characteristic amplitude and period, and approximating them with a model sinusoidal contact line. This treatment provides a complete theoretical description of the meniscus shape and the interparticle force and gives a physical insight about the sign and magnitude of the interaction energy in more complicated cases. In the present chapter we follow the approach from Ref. [1].

Before the theoretical considerations, let us mention some experimental facts, which could be related to the action of the aforementioned capillary force. Heki and Inoue [2] observed the formation of 2-dimensional ordered arrays of μm-sized crystals of silver bromide floating at the air-water interface, see Fig. 12.1. Arrays from hexahedral (cubic) and octahedral crystals were produced, which were separated by areas of bare interface. The latter fact implies that some attractive force has collected the floating microcrystals, which could be the Lucassen's lateral

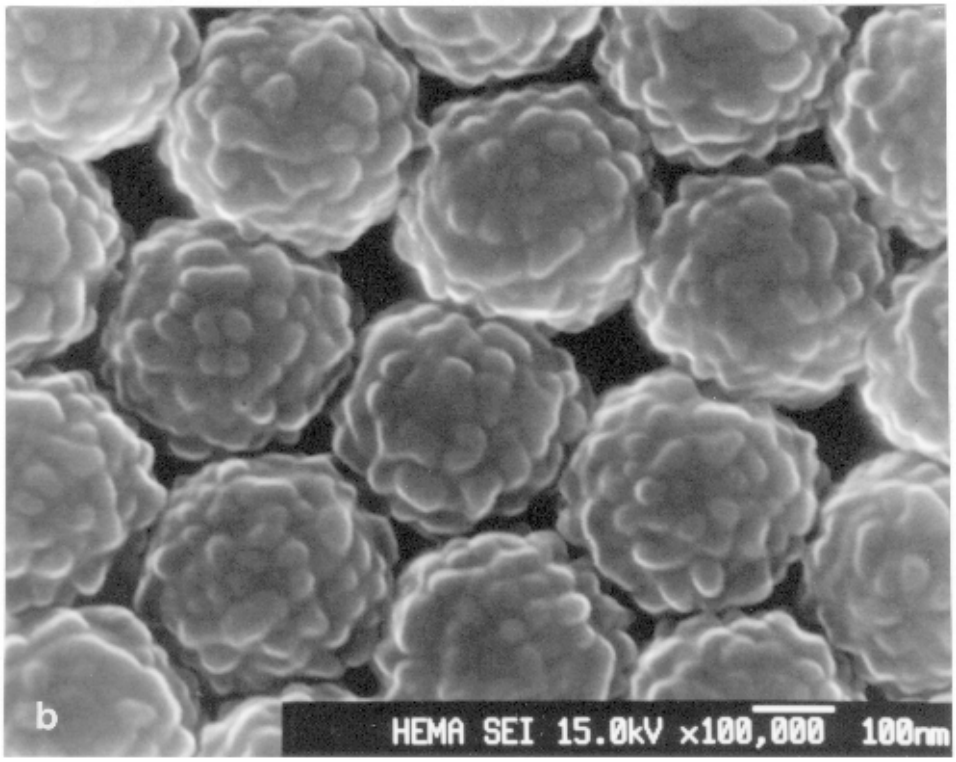

Fig. 12.2. Copolymer latex particles made of polystyrene + 2-hydroxyethyl-metacrylate (PS/HEMA): Secondary electron images of the surface of a colloid crystal obtained by ultra high-resolution-field-emission scanning electron microscope. From Cardoso et al [3], © American Chemical Society; with permission.

capillary force. Other possible explanation could be the attraction due to van der Waals and hydrophobic forces, or the simultaneous action of several kinds of forces.

A contact line of approximately sinusoidal shape can also appear when particles with "undulated" surface are attached to a fluid phase boundary. The spontaneous formation of such particles was observed in the experiments by Cardoso et al. [3], who synthesized latex particles by batch surfactant-free emulsion copolymerization of styrene and 2-hydroxyethyl-metacrylate (PS/HEMA particles), see Fig. 12.2. The properties of 3-dimensional colloid crystals from such particles have been studied by means of electron-microscopic techniques [3].

The model particles used in the theoretical approach of Lucassen, shown in Fig. 12.3, much resemble the cubic microcrystals of silver bromide in Fig. 12.1a. It is assumed that a sinusoidal contact line creates small interfacial deformations, $q\zeta << 1$, where q^{-1} is the capillary length.

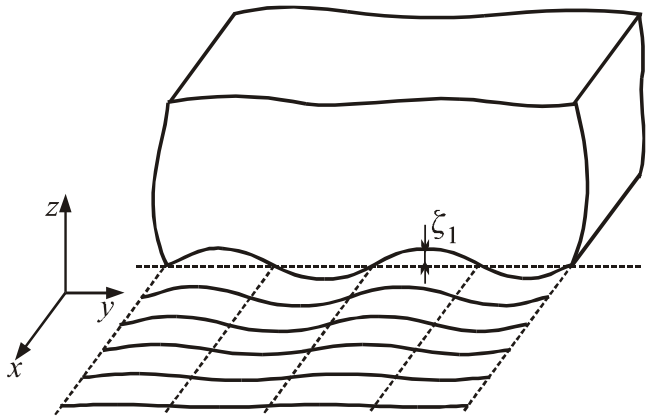

Fig. 12.3. Sketch of a solid particle with sinusoidal contact line located in a plane, which is perpendicular to the x-axis. The undulation of the contact line creates interfacial corrugations, which decay with the increase of the distance x from the particle.

In such case, the right-hand side of the linearized Laplace equation (7.6) can be neglected and one obtains [1]

$$\frac{\partial^2 \zeta}{\partial x^2} + \frac{\partial^2 \zeta}{\partial y^2} = 0 \qquad (q\zeta << 1) \tag{12.1}$$

As known, the general solution of Eq. (12.1) can be presented in the form

$$\zeta(x,y) = \sum_k (A_k \mathrm{e}^{-kx} + B_k \mathrm{e}^{kx})(C_k \sin ky + D_k \cos ky) \tag{12.2}$$

The constants A_k, B_k, C_k and D_k are to be determined from the boundary conditions. For example, if the contact line in Fig. 12.3 has equation $z = \zeta_1 \cos k_1 y$, then the meniscus shape exhibits oscillations, which decay with the distance x from the contact line:

$$\zeta(x,y) = \zeta_1 \exp(-k_1 x) \cos k_1 y \tag{12.3}$$

Here ζ_1 and $\lambda \equiv 2\pi/k_1$ characterize the amplitude and the wavelength of the contact-line undulations. The interfacial corrugations caused by the sinusoidal contact line decay exponentially with the distance x from the edge of the particle. The surface deformation and the capillary interaction are physically significant at distances of the order of, or shorter than, the wavelength $\lambda = 2\pi k_1^{-1}$, see below.

Next, after Lucassen [1], we consider two solid particles floating on a fluid interface (Fig. 12.4) assuming that their sinusoidal edges are parallel to each other and to the y-axis.

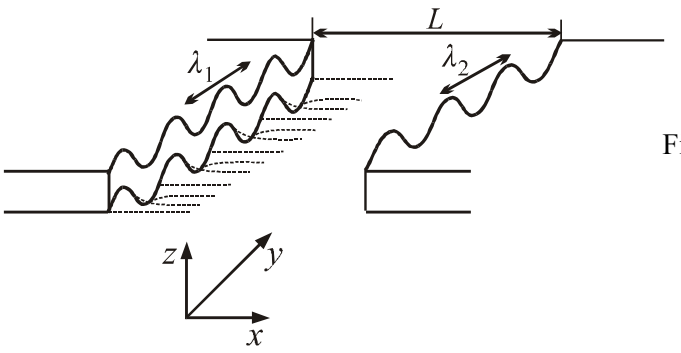

Fig. 12.4. Sketch of two model particles with sinusoidal contact lines belonging to two parallel vertical planes separated at a distance L; λ_1 and λ_2 are the wavelengths of oscillation of the respective contact lines.

The coordinate origin is chosen in the middle between the two particles; in this way their edges are situated at $x = -L/2$ and $x = +L/2$. The equations of the respective contact lines are taken in the form $z = \zeta_1 \cos k_1 y$ and $z = \zeta_2 \cos(k_2 y + \varphi)$, where φ represents a phase difference. Then in view of Eq. (12.2) the shape of the meniscus between the particles is [1]

$$\zeta(x,y) = \zeta_1 \frac{\sinh k_1(L/2 - x)}{\sinh k_1 L} \cos k_1 y + \zeta_2 \frac{\sinh k_2(L/2 + x)}{\sinh k_2 L} \cos(k_2 y + \varphi) \tag{12.4}$$

Equation (12.4) corresponds to the general case of two different amplitudes, ζ_1, ζ_2, and wave numbers, k_1, k_2, in the presence of phase shift φ. On the other hand, the validity of Eq. (12.4) is limited to contact lines lying in two parallel vertical planes (Fig. 12.4).

12.1.2. Energy and force of capillary interaction

As mentioned above, we consider small particles and neglect the gravitational effects. Moreover, the contact lines are fixed to the respective sinusoidal edges (Fig. 12.4), and therefore the energy of wetting does not vary with the interparticle distance L. Then the only nontrivial contribution to the grand thermodynamic potential, Eq. (7.16), originates from the increased area of the corrugated meniscus [1]:

$$\Omega = \sigma \Delta A \approx \frac{\sigma}{2} \int_{-\frac{y_0}{2}}^{\frac{y_0}{2}} dy \int_{-\frac{L}{2}}^{\frac{L}{2}} dx \left[\left(\frac{\partial \zeta}{\partial x} \right)^2 + \left(\frac{\partial \zeta}{\partial y} \right)^2 \right] \tag{12.5}$$

cf. Eq. (7.68). The substitution of Eq. (12.4) into Eq. (12.5) in general gives an explicit analytical expression for Ω. Below we will restrict our considerations to the simpler case of

equal wave numbers, $k_2 = k_1$, and integer number of wave-lengths along the y-axis, $k_1 y_0 = 2\pi n$; $n = 1,2,3,...$. In this case the interaction energy is [1]:

$$\Delta\Omega \equiv \Omega(L) - \Omega(\infty) =$$

$$= \tfrac{1}{4}\pi n\sigma\left[(\zeta_1^2+\zeta_2^2)\left(\coth\frac{k_1L}{2}+\tanh\frac{k_1L}{2}-2\right)-(2\zeta_1\zeta_2\cos\varphi)\left(\coth\frac{k_1L}{2}-\tanh\frac{k_1L}{2}\right)\right] \quad (12.6)$$

The asymptotic form of Eq. (12.6) for long distances, $k_1L >> 1$, reads:

$$\Delta\Omega(L) = -\pi n\sigma\ [(2\zeta_1\zeta_2\cos\varphi)\,\mathrm{e}^{-k_1L} - (\zeta_1^2+\zeta_2^2)\,\mathrm{e}^{-2k_1L} + O(\mathrm{e}^{-3k_1L})] \quad (12.7)$$

Equation (12.7) shows that *at long distances* the interaction is attractive ($\Delta\Omega < 0$) if $\varphi < 90°$, but it is repulsive ($\Delta\Omega > 0$) if $\varphi \geq 90°$. On the other hand, *at short distances*, $k_1L << 1$, Eq. (12.6) is dominated by the hyperbolic cotangent:

$$\Delta\Omega(L) = \tfrac{1}{2}\pi n\sigma\ \left[(\zeta_1^2+\zeta_2^2 - 2\zeta_1\zeta_2\cos\varphi)\frac{1}{k_1L} - (\zeta_1^2+\zeta_2^2) + O(k_1L)\right] \quad (12.8)$$

Equation (12.8) implies that at short distances the capillary interaction is always repulsive ($\Delta\Omega > 0$). An exception is the very special case, in which simultaneously $\zeta_1 = \zeta_2$, $\varphi = 0$ and the terms with hyperbolic cotangents cancel each other; in this case the interaction is attractive for all distances.

The above analysis implies that for $\varphi < 90°$ $\Delta\Omega(L)$ has a minimum at a certain distance $L_{\min}$, which can be found from Eq. (12.7) [1]:

$$L_{\min} = \frac{1}{k_1}\operatorname{arc\,cosh}\left(\frac{\zeta_1^2+\zeta_2^2}{2\zeta_1\zeta_2\cos\varphi}\right) \quad (12.9)$$

This minimum, corresponding to equilibrium interparticle separation, exists for $-90° < \varphi < 90°$, but it disappears for larger phase shift, $90° \leq \varphi \leq 270°$. Special cases of Eq. (12.9) are

$$L_{\min} = \frac{1}{k_1}\,|\ln(\zeta_1/\zeta_2)| \qquad \text{for } \varphi = 0 \quad (12.10)$$

$$L_{\min} = \frac{1}{k_1}\ln\left(\frac{1+\sin\varphi}{\cos\varphi}\right) \qquad \text{for } \zeta_1 = \zeta_2 \quad (12.11)$$

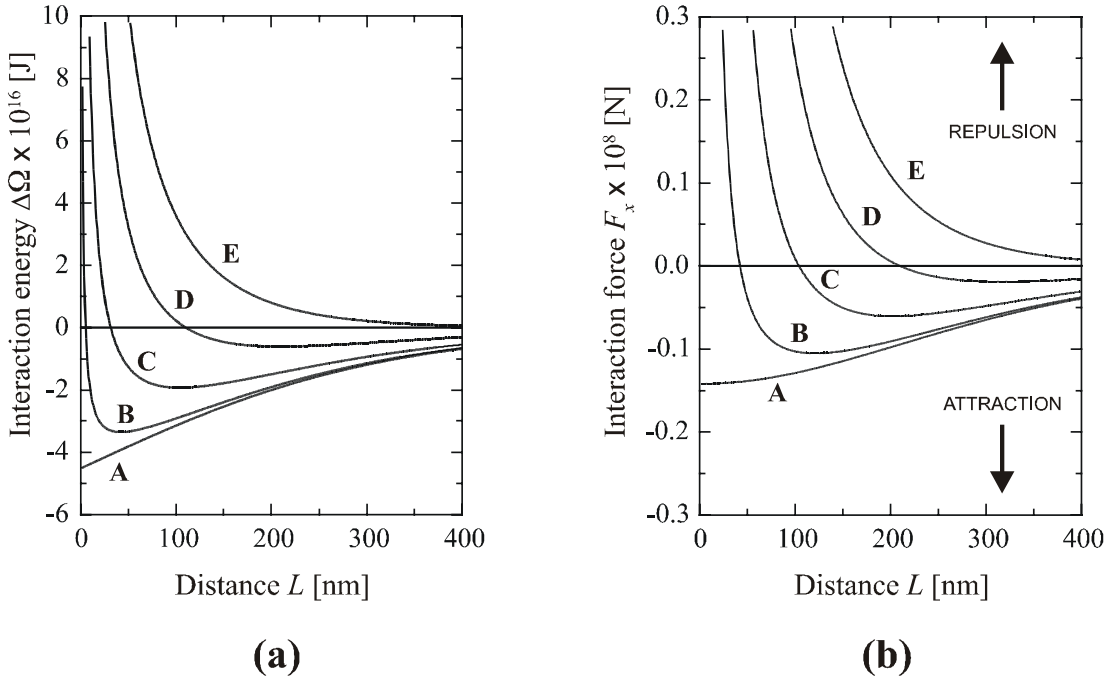

Fig. 12.5. Plots of (a) energy $\Delta\Omega$ and (b) force F_x vs. distance L, calculated by means of Eqs. (12.6) and (12.12) for λ = 1 μm, n = 1, σ = 40 mN/m and ζ_1 = ζ_2 = 60 nm; the separate curves correspond to the following values of the phase-shift angle: (A) φ = 0, (B) φ = 15°, (C) φ = 35°, (D) φ = 60° and (E) φ = 90°.

The force between the two particles can be deduced by differentiation of Eq. (12.6) [1]:

$$F_x = -\frac{\partial \Delta\Omega}{\partial L} = \tfrac{1}{8}\pi n\sigma k_1 \left[\frac{\zeta_1^2 + \zeta_2^2 - 2\zeta_1\zeta_2\cos\varphi}{\sinh^2(k_1 L/2)} - \frac{\zeta_1^2 + \zeta_2^2 + 2\zeta_1\zeta_2\cos\varphi}{\cosh^2(k_1 L/2)} \right] \tag{12.12}$$

The dependence of $\Delta\Omega$ on the phase angle φ leads to the appearance of a force component also along the y-axis [1]:

$$F_y = -\frac{\partial \Delta\Omega}{k_1^{-1}\partial\varphi} = -\tfrac{1}{2}\pi n\sigma k_1 \zeta_1\zeta_2 \sin\varphi \left(\coth\frac{k_1 L}{2} - \tanh\frac{k_1 L}{2} \right) \tag{12.13}$$

F_y is a force which tends to make the particles slide with respect to one another in a direction parallel to the y-axis. The action of this force will eventually bring the particles in a position without phase shift, i.e. with φ = 0. In the latter case the expression for the interaction energy, Eq. (12.6), reduces to

$$\Delta\Omega = \tfrac{1}{4}\pi n\sigma \left[(\zeta_1 + \zeta_2)^2 \tanh(k_1 L/2) + (\zeta_1 - \zeta_2)^2 \coth(k_1 L/2) - 2(\zeta_1^2 + \zeta_2^2) \right] \tag{12.14}$$

The minimum value of $\Delta\Omega$ can be obtained substituting Eq. (12.10) into Eq. (12.14). Let us specify that $\zeta_2 \le \zeta_1$. Then one obtains

$$\tanh(k_1 L_{\min}/2) = \frac{\zeta_1 - \zeta_2}{\zeta_1 + \zeta_2} = [\coth(k_1 L_{\min}/2)]^{-1} \qquad (\varphi = 0,\ \zeta_2 \le \zeta_1) \qquad (12.15)$$

$$\Delta\Omega_{\min} \equiv \Delta\Omega(L_{\min}) = -\pi n \sigma \zeta_2^2 \qquad (\varphi = 0,\ \zeta_2 \le \zeta_1) \qquad (12.16)$$

Let us check whether the depth of the minimum, $|\Delta\Omega_{\min}|$, is significant compared with the energy of the thermal motion of a Brownian particle, which is approximately equal to kT. The value of the amplitude ζ_2 , which provides $\Delta\Omega_{\min} \approx kT$, is $\zeta_2 = (kT/\pi n\sigma)^{1/2}$; taking surface tension $\sigma = 40$ mN/m, temperature 25°C and n =1 (the length of the particle equals 1 wave-length) one calculates $\zeta_2 = 1.8$ Å. This result is really astonishing: it turns out that even edge irregularities of angstrom amplitude may lead to physically significant attraction between the particles! However, in the angstrom scale the fluid interfaces are no longer smooth: they are naturally corrugated by thermally excited fluctuation capillary waves, whose amplitude is typically between 3 and 6 Å [4]. Then one can expect that the effect of the undulated particle contact lines becomes significant when the amplitude of the undulations is greater than this stochastic noise, that is for nanometer and larger amplitudes. In any case, one may expect that such capillary interactions could be important even for large adsorbed macromolecules of irregular shape, like the proteins.

Figure 12.5a shows the dependence of the interaction energy $\Delta\Omega$ on the distance L calculated by means of Eq. (12.6) for four different values of the phase angle φ; for all curves n = 1, $\lambda \equiv 2\pi/k_1$ = 1 μm and the amplitudes of the two sinusoidal contact lines are equal: $\zeta_1 = \zeta_2 =$ 60 nm. As noted above, the interaction is monotonic attraction at all distances only if simultaneously $\varphi = 0$ and $\zeta_1 = \zeta_2$. For $0 < \varphi < 90°$ the curves exhibit minima at $L = L_{\min}$, see Eq. (12.11) and Fig. 12.5a. For $90° \le \varphi \le 270°$ the interaction is monotonic repulsion. The magnitude of interaction at short separations (L < 500 nm) is much larger than the thermal energy kT. For example, for the curve with $\varphi = 0$ the magnitude of the energy $|\Delta\Omega|$ is equal to $1.1 \times 10^5\ kT$ at close contact (L = 0), and it drops down to 1 kT at a separation $L \approx 2.0$ μm = 2λ.

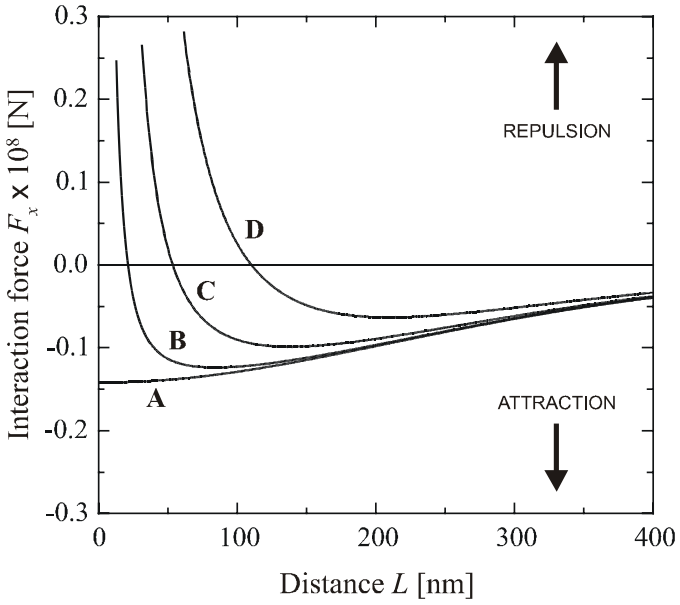

Fig. 12.6. Plots of the lateral capillary force F_x vs. distance L, calculated by means of Eq. (12.12) for $\lambda = 1$ μm, $n = 1$, $\sigma = 40$ mN/m and $\varphi = 0$; the separate curves correspond to (A) $\zeta_1 = 60$ nm, $\zeta_2 = 60$ nm; (B) $\zeta_1 = 56$ nm, $\zeta_2 = 64$ nm; (C) $\zeta_1 = 50$ nm, $\zeta_2 = 70$ nm; (D) $\zeta_1 = 40$ nm, $\zeta_2 = 80$ nm.

Figure 12.5b presents the dependence of force F_x on distance L calculated by means of Eq. (12.12) for the same values of the parameters as in Fig. 12.5a. The points with $F_x = 0$ correspond to the equilibrium separation between two particles. One sees again that the interaction becomes more repulsive with the rise of the phase shift φ.

Figure 12.6 illustrates the tendency the interaction to become more repulsive when the difference between the amplitudes ζ_1 and ζ_2 increases. For example, a difference $\zeta_1 - \zeta_2 \approx 5$ nm produces the same effect as a phase shift $\varphi \approx 10°$. In Fig. 12.6 we have fixed $\varphi = 0$, and consequently, the interaction is attractive at *long* distances for every values of ζ_1 and ζ_2.

12.2. ELASTIC PROPERTIES OF PARTICULATE ADSORPTION MONOLAYERS

The fact that the capillary interaction energy $\Delta\Omega(L)$ has a minimum leads to the appearance of elastic behavior of a fluid interface covered by "rough-edged" particles (i.e. particles with corrugated contact line). As noted by Lucassen [1], any deformation of this surface, either by dilatation or by shear, will take the particles out of their equilibrium positions and will, therefore, be resisted. As a consequence, the particulate monolayer will exhibit dilatational and shear elastic properties.

12.2.1. SURFACE DILATATIONAL ELASTICITY

Let us consider a fluid surface covered with square particles of edge length $y_0 = \lambda = 2\pi/k_1$. It is natural to assume that the particles spontaneously adjust their lateral positions so that $F_y = 0$ and consequently, $\varphi = 0$. Let us denote the area per particle in the monolayer with a. Then the surface dilatational elasticity of the particulate monolayer can be defined in the same way as for surfactant molecules:

$$E_G = a\frac{d\sigma_{\text{ap}}}{da} \tag{12.17}$$

cf. Eq. (1.45); here σ_{ap} is the apparent surface tension of the particulate monolayer. For our rectangular particles of edge-length λ separated at edge-to-edge distance L one has $a = (\lambda + L)^2$. Then $da = 2(\lambda + L)dL$ and Eq. (12.17) acquires the form

$$E_G = \tfrac{1}{2}(\lambda + L)\frac{d\sigma_{\text{ap}}}{dL} \approx \tfrac{1}{2}\lambda\frac{d\sigma_{\text{ap}}}{dL} \approx \frac{1}{2}\left|\frac{dF_x}{dL}\right| \qquad (L << \lambda) \tag{12.18}$$

where at the last step we have identified the variation of the apparent surface tension with the increment of F_x per unit length, i.e. $d\sigma_{\text{ap}} \approx |dF_x|/\lambda$. Setting $\varphi = 0$ in Eq. (12.12) and differentiating one obtains

$$\frac{dF_x}{dL} = -\tfrac{1}{8}\pi\sigma k_1^2\left[\left(\zeta_1 - \zeta_2\right)^2\frac{\coth(k_1L/2)}{\sinh^2(k_1L/2)} - \left(\zeta_1 + \zeta_2\right)^2\frac{\tanh(k_1L/2)}{\cosh^2(k_1L/2)}\right] \tag{12.19}$$

As already mentioned, we consider small deviations from the equilibrium position of the particles. Then setting $L = L_{\min}$ in Eq. (12.19) and using Eqs. (12.15) and (12.18) we derive

$$\frac{dF_x}{dL} = -2\pi\sigma\frac{k_1^2\zeta_1^2\zeta_2^2}{\zeta_1^2 - \zeta_2^2} \qquad (L = L_{\min}) \tag{12.20}$$

Let us denote by ζ_0 and $\Delta\zeta$, respectively, the average value and the dispersion of the amplitude of the contact-line undulations for the particles from the adsorption monolayer; we will assume $\Delta\zeta << \zeta_0$. Then combining Eqs. (12.18) and (12.20) we obtain an estimate for the surface *dilatational elasticity*:

$$E_G \approx \frac{2\pi^3\sigma\zeta_0^3}{\lambda^2\Delta\zeta} \tag{12.21}$$

where the identity $k_1 = 2\pi/\lambda$ has been used. Note that the surface dilatational elasticity E_G is sensitive to both ζ_0 and $\Delta\zeta$. With values $\sigma = 40$ mN/m, $\lambda = 1$ μm, $\zeta_0 = 60$ nm and $\Delta\zeta = 6$ nm Eq. (12.21) gives $E_G \approx 89$ mN/m; this is a considerable value, which is comparable with the surface elasticity of surfactant adsorption monolayers.

The divergence of E_G for $\Delta\zeta \to 0$ is related to the fact that in the limit $\Delta\zeta \to 0$ the particles come into direct contact ($L_{\min} = 0$). Indeed, with $\Delta\zeta = \zeta_1 - \zeta_2$ Eq. (12.10) yields

$$L_{\min} \approx \Delta\zeta / \zeta_0 \qquad (\Delta\zeta << \zeta_0) \tag{12.22}$$

12.2.2. SURFACE SHEAR ELASTICITY

Let us consider again an equilibrium monolayer of square "rough-edged" particles having side-length λ. A small shear deformation along the y-axis (Fig. 12.4) is accompanied by the appearance of a shear stress:

$$\tau_{\rm sh} = E_{\rm sh} \frac{\Delta u_y}{\Delta x} \approx E_{\rm sh} \frac{\varphi / k_1}{L_{\min}} \tag{12.23}$$

where $E_{\rm sh}$ is the surface shear elasticity, $\Delta u_y \approx \varphi / k_1$ is a small relative particle displacement along the y-axis, and $\Delta x = L_{\min}$ is the equilibrium separation between the edges of the two particles along the x-axis; see e.g. Ref. [5]. For small displacements (small φ) one can estimate the surface shear stress $\tau_{\rm sh}$ with the help of Eq. (12.13):

$$\tau_{\rm sh} = -F_y / \lambda = \tfrac{1}{2} \pi \sigma k_1 \varphi \zeta_1 \zeta_2 \left(\coth \frac{k_1 L_{\min}}{2} - \tanh \frac{k_1 L_{\min}}{2} \right) \tag{12.24}$$

Combining Eqs. (12.23) and (12.24), along with Eqs. (12.10), (12.15) and (12.22), after some transformations we obtain the following expression for the surface *shear elasticity*:

$$E_{\rm sh} \approx 2\pi^2 \sigma (\zeta_0 / \lambda)^2 \tag{12.25}$$

where the meaning of ζ_0 and λ is the same as in Eq. (12.21). The comparison of Eqs. (12.21) and (12.25) shows that, unlike the dilatational elasticity E_G, the shear elasticity $E_{\rm sh}$ does not depend on the dispersion $\Delta\zeta$ of the amplitudes of the particle edge roughness. With $\sigma =$ 40 mN/m and $\zeta_0/\lambda = 0.1$ Eq. (12.25) yields $E_{\rm sh} \approx 8$ mN/m.

Equation (12.25) has been derived for the case of small shear displacements, for which we can substitute $\sin\varphi \approx \varphi$ in Eq. (12.13); i.e. we have dealt with small deviations from the state of

minimum energy. For larger shear displacements the interaction energy $\Delta\Omega$ passes through a *maximum* (barrier) at $\varphi = \pi$, which should be overcome by the particles in order to have a viscous shear flow in the interface [6]. The height of this barrier, U_m, can be estimated by means of Eq. (12.6)

$$U_m \equiv \Delta\Omega(\varphi = \pi) - \Delta\Omega(\varphi = 0) = \pi\sigma\zeta_1\zeta_2 \left(\coth\frac{k_1 L}{2} - \tanh\frac{k_1 L}{2} \right) \tag{12.26}$$

The coverage of the fluid interface with square particles of edge λ is $\alpha \equiv \lambda^2/(\lambda + L)^2$. Using the latter relationship and $k_1 = 2\pi/\lambda$ one obtains

$$k_1 L = \pi(\alpha^{-1/2} - 1) \tag{12.27}$$

Using Eqs. (12.26), (12.27) and the values $\alpha = 0.8$, $\zeta_1 = \zeta_2 = 60$ nm and $\sigma = 40$ mN/m one calculates $U_m \approx 2.7 \times 10^5\ kT$. It seems that such a high energy barrier will prevent any surface shear flow (the surface viscosity is $\eta_s \propto \exp(U_m/kT)$, see Ref. [6]), and consequently, the particulate monolayer will behave as an elastic two-dimensional continuum. Note however, that the expression for the height of the barrier Eq. (12.26), is obtained assuming a *translational* slip along the *y*-axis. However, in reality each particle is free to *rotate* around its axis, and this fact certainly increases the interfacial fluidity. The estimate of the surface *shear viscosity* based on account for the particle rotation is out of the applicability range of the present simple model with square particles.

12.3. SUMMARY

The contact line of a solid particle attached to a fluid interface may have irregular shape due to surface roughness or inhomogeneity. Such an irregular contact line corrugates the surrounding fluid interface. The overlap of the corrugations around two particles gives rise to a lateral capillary force between them. A quantitative theoretical description of this effect was given by Lucassen [1] who considered irregularities of a given characteristic amplitude and period, and approximated them with a model sinusoidal contact line, Fig. 12.3 and Eq. (12.3). Assuming that the sinusoidal contact lines of the two interacting particles belong to two parallel vertical planes, one can derive an analytical expression for the meniscus shape, Eq. (12.4).

In general, the corrugations increase the interfacial area. When the approaching of two particles causes decreasing of the interfacial area, the interparticle force is attractive; in the opposite case (increasing of the area) the particles repel each other. The latter effects are quantified by Eq. (12.6). If the phase shift φ between the two sinusoidal contact lines is not too

large ($0 \le \varphi < 90°$) the interaction is always attractive at long distances between the particles, see Eq. (12.7). On the other hand, at short distances the interaction is always repulsive, see Eq. (12.8) and Figs. 12.5 and 12.6. The only exclusion (monotonic attraction at all distances) is the case, in which there is no phase shift ($\varphi = 0$), and moreover, the amplitudes are identical ($\zeta_1 = \zeta_2$).

The interaction energy exhibits a minimum at some interparticle separation L_{min}, given by Eqs. (12.9)–(12.11). The depth of the minimum turns out to be greater than the thermal energy kT even for contact-line undulations of nanometer amplitude, see Eq. (12.16). This striking fact implies that the considered type of capillary force could be significant even between nanoparticles and protein macromolecules, and that its physical importance should not be neglected.

Any deformation of a particulate adsorption monolayer, either by dilatation or by shear, which takes the particles out of their equilibrium positions, is resisted. As a result the particle monolayer exhibits dilatational and shear elasticity, which can be estimated by means of Eqs. (12.21) and (12.25) knowing the average value, ζ_0, and the dispersion, $\Delta\zeta$, of the amplitude of the contact-line undulations.

12.4. REFERENCES

1. J. Lucassen, Colloids Surf. 65 (1992) 131.
2. T. Heki, N. Inoue, Forma 4 (1989) 55.
3. A.H. Cardoso, C.A.P. Leite, F. Galembeck, Langmuir 15 (1999) 4447.
4. J.S. Rowlinson, B. Widom, Molecular Theory of Capillarity, Clarendon Press, Oxford, 1982.
5. E.S. Basheva, A.D. Nikolov, P.A. Kralchevsky, I.B. Ivanov, D.T. Wasan, in: K.L. Mittal and D.O. Shah (Ed.) Surfactants in Solution, Vol. 11, Plenum Press, New York, 1991.
6. J. Frenkel, Kinetic Theory of Liquids, Clarendon Press, Oxford, 1946.

For new developments on interactions between particles of undulated contact line see also:
1. A.B.D. Brown, C.G. Smith, A.R. Rennie, Fabricating colloidal particles with photolithography and their interactions at air-water interface. Phys. Rev. E, 62 (2000) 951-960.
2. D. Stamou, C. Duschl, D. Johannsmann, Long-range attraction between colloidal spheres at the air-water interface: The consequence of an irregular meniscus. Phys. Rev. E, 62 (2000) 5263-5272.
3. P.A. Kralchevsky, N.D. Denkov, Capillary forces and structuring in layers of colloid particles. Curr. Opin. Colloid Interf. Sci. 6 (2001) 383–401.
4. P. A. Kralchevsky, N. D. Denkov, K. D. Danov, Particles with undulated contact line at a fluid interface: Interaction between capillary quadrupoles and rheology of particulate monolayers", Langmuir 17 (2001) 7694–7705.